Ocean Systems Engineering, *Vol. 3, No. 4 (2013) 257-273*
DOI: http://dx.doi.org/10.12989/ose.2013.3.4.257

Numerical model of a tensioner system and riser guide

Han Huang[1], Jun Zhang[*2] and Liyun Zhu[2]

[1]*Offshore Engineering Department, American Bureau of Shipping, Houston, TX, USA*
[2]*Ocean Engineering Program, Civil Engineering Department, Texas A&M University, College Station, TX, USA*

(Received Sptember 28, 2013, Revised October 20, 2013, Accepted October 25, 2013)

Abstract. Top tensioned riser (TTR) is often used in a floating oil/gas production system deployed in deep water for oil/gas transport. This study focuses on the extension of the existing numerical code, known as CABLE3D, to allow for static and dynamic simulation of a TTR connected to a floating structure through a tensioner system or buoyancy can, and restrained by riser guides at different elevations. A tensioner system usually consists of three to six cylindrical tensioners. Although the stiffness of individual tensioner is assumed to be linear, the resultant stiffness of a tensioner system may be nonlinear. The vertical friction between a TTR and the hull at its riser guide is neglected assuming rollers are installed there. Near the water surface, a TTR is forced to move horizontally due to the motion of the upper deck of a floating structure as well as related riser guides. The extended CABLE3D is then integrated into a numerical code, known as COUPLE, for the simulation of the dynamic interaction among the hull of a floating structure, such as spar or TLP, its mooring system and riser system under the impact of wind, current and waves. To demonstrate the application of the extended CABLE3D and its integration with COUPLE, the numerical simulation is made for a truss spar under the impact of Hurricane 'Ike'. The mooring system of the spar consists of nine mooring lines and the riser system consists of six TTRs and two steel catenary risers (SCRs).

Keywords: dynamic simulation; top tensioned riser; tensioner; riser guide; cable3D; COUPLE

1. Introduction

Different types of offshore platforms are employed for better performance as oil and gas exploration is pushed into deeper and deeper water (Murray *et al.* 2007). On floating host platforms, dry-tree systems are constructed to facilitate tieback of the subsea manifolds, via TTRs, to minimize the construction and production costs (Murray *et al.* 2006). The top tension of a TTR is provided by either a buoyancy can or a deck mounted tensioner system, such as hydropneumatic tensioner (Yang and Kim 2010, 2011). Both types of TTR are used in various kinds of platforms, including tension leg platforms (TLPs), semi-submersible and spars.

On a TLP, a TTR with a tensioner system is more widely utilized. Whilst on a spar deployed in moderate-depth water, a TTR with a buoyancy can is more popular. In the latter case, buoyancy cans are installed to provide tension at the top of production and drilling risers. A TTR tensioned by a buoyancy can does not impose vertical loads on the spar hull and its vertical movement is virtually independent of the hull motion (Chen *et al.* 2008). However for spars that are deployed at

*Corresponding author, Professor, E-mail: jzhang@civil.tamu.edu

http://www.techno-press.org/?journal=ose&subpage=7 ISSN: 2093-6702 (Print), 2093-677X (Online)

ultra-deep water depth (>1500 m), disadvantages of TTRs of this kind begin to emerge. As water depth increases, the volume of a buoyancy can becomes greater due to the increase in the weight of a TTR. Because of the limited size of the moon pool of a spar, the buoyancy can design might not be a feasible choice under the ultra-deep water circumstance (Chen *et al.* 2008).

Because the technology in making tensioners has advanced significantly recently, tensioners show greater advantages in comparison of buoyancy cans, especially for ultra-deep water conditions. Although tensioners avoid negative effects on the center well and spar hull size, they will exert tension loads on the floating structure and also have a functional constraint owing to limited strokes of tensioner (Chen *et al.* 2008). Advances in tensioner technology make the larger stroke available. Hence TTRs tensioned by tensioner systems are increasingly gaining popularity in real-world applications. Therefore, the global performance analysis of TTRs of such type is of great significance to their design.

For the purposes mentioned above, several extensions are made to the existing numerical code, CABLE3D, to allow for static and dynamic simulation of a TTR connected to a floating structure through either a tensioner system or a buoyancy can, and with riser guides at different elevations near the water surface. The extended CABLE3D are then integrated into a numerical code, COUPLE, for the simulation of the dynamic interaction among the hull of a spar, its mooring system and riser system under the impact of wind, current and waves.

2. Numerical models

2.1 Risers

TTRs could be modeled as small extensible slender rods with given bending stiffness. The equations for motion of slender rods mainly follow the work by Love (1944), Nordgren (1974), Garrett (1982), Paulling and Webster (1986), Ma and Webster (1994) and Chen (2002). When there is no external torque and moment applied on a mooring line/riser, the governing equation for its motion can be expressed as

$$-(B\mathbf{r}'')'' + (\lambda \mathbf{r}')' + \mathbf{q} = \rho \ddot{\mathbf{r}} \tag{1}$$

where **r** represents the position vector along a riser, which is function of arc length s and time t; the prime denotes the derivatives with respect to *s* and a superposed dot denotes differentiation with respect to time. *B* represents the bending stiffness, **q** the distributed external force per unit length, and ρ the mass per unit length. The scalar variable λ is defined below

$$\lambda = T - B\kappa^2 \tag{2}$$

where κ is the local curvature of the rod, and $T(s,t) = \mathbf{r}' \cdot \mathbf{F}$ is the local tension. Besides, r must satisfy a stretching constant equation

$$\mathbf{r}' \cdot \mathbf{r}' = (1 + \frac{T}{EA})^2 \tag{3}$$

where *EA* is the elastic stiffness of the riser.

The external forces **q** applied on the riser include gravity forces, hydrostatic and

hydrodynamic forces which are calculated using the Morrison equation. Combined with the initial conditions and boundary conditions, the governing equations Eqs. (1) and (3), can be solved numerically using a finite element method (FEM). The kinematic boundary condition at the upper end of each mooring line/riser is imposed by the description of the relative motion at the fairlead/porch. The dynamic boundary condition is that the total summation of all mooring line top tension, SCR top tension, forces provided by tensioner system and riser guides is equal to their force applied on the spar. If the connection between the SCR and the spar is a flex-joint, a bending moment is applied at the porch of the SCR.

The Galerkin's method is adopted to discretize the partial differential equations of motion from (1), and the constraints equation shown in Eq. (3), resulting in a set of nonlinear 2nd-order ordinary differential equations in the time domain. Following Chen (2002), Newton's method and Newmark-β method were employed to solve the static problem and dynamic problem, respectively.

Using the matching conditions between a floating structure and its mooring/riser system, the dynamic equations for the coupled system can be solved simultaneously in the time domain.

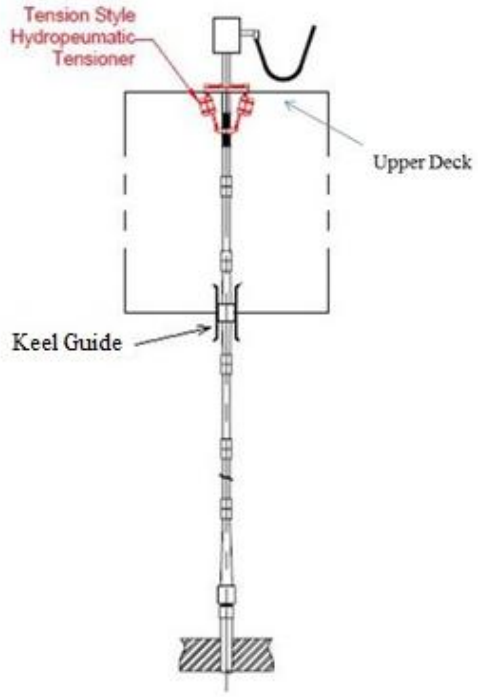

Fig. 1 Configuration of upper deck, tensioner system and riser guide (Perryman *et al.* 2005)

2.2 Tensioner systems

The configuration of a typical TTR is depicted in Fig. 1. A tensioner system may consist of three to six individual cylindrical tensioners. The tension of an individual tensioner cylinder is

approximated by a linear spring in this study. Although the tension provided by an individual tensioner is linear, the stiffness of the whole tensioner system is likely to be nonlinear. When the concentrated force ($\tilde{\mathbf{f}}$) provided by a tensioner system is applied at s_0 along a slender rod, the corresponding force can be added to the dynamic equations by introducing a δ function as follows (Chen 2002)

$$\mathbf{M}\ddot{\mathbf{r}} + (B\mathbf{r}'')'' - (\tilde{\lambda}\mathbf{r}')' - \mathbf{q} + \delta(s - s_0)\left\{-\tilde{\mathbf{f}}\right\} = 0 \tag{4}$$

The tension of each tensioner cylinder at each time step is given by

$$\left|\vec{f}_i\right| = \left|\vec{f}_{0i}\right| + k_i(L_i - L_{0i}) \tag{5}$$

where $\vec{f}_i$ represents the tension of the *i*th tensioner and the subscript, *i*, specifies an individual tensioner. Its 'spring' stiffness is denoted by k_i, the initial pretension by $\vec{f}_{0i}$, and the initial length by L_{0i}. The length of a tensioner at a given time step is L_i. The computation of L_i and L_{0i} is given in Eqs. (6) and (7).

$$L_i = \left|\vec{D}_i - (\vec{r}_i + \delta\vec{r}_i)\right| \tag{6}$$

$$L_{0i} = \left|\vec{D}_{0i} - \vec{r}_{0i}\right| \tag{7}$$

where $\vec{D}_i$ represents the coordinates of the upper end of a tensioner, which describe the location of its connection to the upper deck; $\vec{r}_i$ is the coordinates of the lower end of the tensioner, which describe the location of the connection between a tensioner and riser, at a given time step. $\vec{D}_{0i}$ is the initial position of the upper end of *i*th tensioner while $\vec{r}_{0i}$ represents the initial position of the lower end of the tensioner. $\delta\vec{r}_i$ is the unknown increment of $\vec{r}_i$ at each time step and will be calculated in solving the global equation. Thus $\vec{r}_i + \delta\vec{r}$ is the predictor of the coordinates at each time step.

The three components of the force, $\vec{f}_i$, in the *x*, *y*, *z* directions can be obtained by introducing a unit direction vector $\vec{d}_i$, which is given in the following formula.

$$\vec{d}_i = \frac{\vec{D}_i - (\vec{r}_i + \delta\vec{r}_i)}{\left|\vec{D}_i - (\vec{r}_i + \delta\vec{r}_i)\right|} \tag{8}$$

Using the Taylor expansion and neglecting the high-order terms involving $\delta\vec{r}_i$, the expressions for $\left|\vec{f}_i\right|$ and $\vec{d}_i$ can be obtained. By introducing $f_{ij} = \left|f_i\right| d_{ij}$, the three components of $\vec{f}_i$ are obtained in Eqs. (9)- (11).

$$f_{i1} = T_i \frac{D_{i1} - r_{i1}}{l_i} \begin{Bmatrix} 1 + \left[\frac{D_{i1} - r_{i1}}{l_i^{\,2}} - \frac{k_i (D_{i1} - r_{i1})}{T_i l_i} - \frac{1}{D_{i1} - r_{i1}} \right] \delta r_{i1} + \\ \left[\frac{D_{i2} - r_{i2}}{l_i^{\,2}} - \frac{k_i (D_{i2} - r_{i2})}{T_i l_i} \right] \delta r_{i2} + \left[\frac{D_{i3} - r_{i3}}{l_i^{\,2}} - \frac{k_i (D_{i3} - r_{i3})}{T_i l_i} \right] \delta r_{i3} \end{Bmatrix} \tag{9}$$

$$f_{i2} = T_i \frac{D_{i2} - r_{i2}}{l_i} \begin{Bmatrix} 1 + \left[\frac{D_{i1} - r_{i1}}{l_i^{\,2}} - \frac{k_i (D_{i1} - r_{i1})}{T_i l_i} \right] \delta r_{i1} + \\ \left[\frac{D_{i2} - r_{i2}}{l_i^{\,2}} - \frac{k_i (D_{i2} - r_{i2})}{T_i l_i} - \frac{1}{D_{i2} - r_{i2}} \right] \delta r_{i2} + \left[\frac{D_{i3} - r_{i3}}{l_i^{\,2}} - \frac{k_i (D_{i3} - r_{i3})}{T_i l_i} \right] \delta r_{i3} \end{Bmatrix} \tag{10}$$

$$f_{i3} = T_i \frac{D_{i3} - r_{i3}}{l_i} \begin{Bmatrix} 1 + \left[\frac{D_{i1} - r_{i1}}{l_i^{\,2}} - \frac{k_i (D_{i1} - r_{i1})}{T_i l_i} \right] \delta r_{i1} + \\ \left[\frac{D_{i2} - r_{i2}}{l_i^{\,2}} - \frac{k_i (D_{i2} - r_{i2})}{T_i l_i} \right] \delta r_{i2} + \left[\frac{D_{i3} - r_{i3}}{l_i^{\,2}} - \frac{k_i (D_{i3} - r_{i3})}{T_i l_i} - \frac{1}{D_{i3} - r_{i3}} \right] \delta r_{i3} \end{Bmatrix} \tag{11}$$

where $T_i = \left| \vec{f}_{0i} \right| + k_i \left(l_i - \left| \vec{D}_{0i} - \vec{r}_{0i} \right| \right)$ and $l_i = \left[(D_{i1} - r_{i1})^2 + (D_{i2} - r_{i2})^2 + (D_{i3} - r_{i3})^2 \right]^{1/2}$.

Substituting the expressions of f_{ij} into the global equation system and moving the terms involving $\delta \vec{r}_i$ to the left hand side of the global equations, we have considered the effects of a tensioner system in the dynamic analysis of a TTR.

2.3 Buoyancy cans

For TTRs tensioned by buoyancy cans, the top tension of a TTR is provided by the buoyancy can attached at its top. In addition, a TTR is laterally constrained by its riser guides at several elevations inside the hull of a spar but is allowed to move independently in the vertical direction (Chen and Nurtjahyo 2004). The buoyancy is constant because of the constant volume of a buoyancy can and the virtually constant water level inside a moon pool. The approach of modeling a buoyancy can is to introduce different element types while discretizing the riser. For elements located within the buoyancy can segment, the additional buoyancy provided by a buoyancy can is added to their total buoyancy, which is the input of CABLE3D.

2.4 Riser guides

Due to its motion, the hull applies forces on the TTRs through the upper deck and riser guides. As mentioned earlier, the vertical friction between TTRs and the upper deck or riser guides is neglected. As shown in Fig. 1, the upper deck locates at the top of tensioner system and the riser guides are often below the sea surface. The lowest riser guide is called the keel guide. A TTR is restrained by riser guides in the horizontal directions. Hence, it is necessary to know the instant locations of the upper deck and related riser guides in order to simulate the TTR motion. Since a

TTR moves with respect to riser guides in vertical direction, the locations of contact between the TTR and its riser guides may vary along the TTR at different time steps.

Translation and rotation motions of a floating platform are considered to determine the instant locations of the riser guides. The relationship between space-fixed coordinates $\hat{\mathbf{x}} = (\hat{x}, \hat{y}, \hat{z})^t$ and body-fixed coordinates $\mathbf{x} = (x, y, z)^t$ is related in Eq. (12) (Chen 2002)

$$\hat{\mathbf{x}} = \boldsymbol{\xi} + \mathbf{T}^t \mathbf{x} \tag{12}$$

where $\boldsymbol{\xi} = (\xi_1, \xi_2, \xi_3)^t$, is the translation displacement of the hull expressed in the space fixed coordinate system, $\mathbf{T}$ is a transfer matrix between body-fixed coordinate system and the space-fixed coordinate system, superscript t represents transpose of a matrix.

Since the body-fixed coordinates of upper deck and riser guides are known in advance, their instant location can be calculated using (12). The motion of the spar determines the locations of the riser guides, and the locations of riser guides are transmitted from the main program COUPLE to CABLE3D subroutine as an excitation. As a return, the forces and moments applied by TTRs on the hull at the locations of riser guides are fed back to the main program for the simulation of the motion of the hull.

3. Background of 'Constitution' spar

3.1 Principal dimensions

After the extended CABLE3D is integrated into COUPLE, COUPLE is applicable to the analysis of a floating system consisting of a hull, mooring system, SCRs and TTRs. 'Constitution', a truss spar, is selected for the demonstration of the numerical simulation using the extended COUPLE. The spar is sketched in Fig. 2 and its characteristics are listed in Table 1.

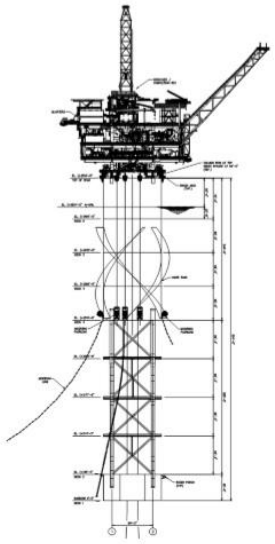

Fig. 2 Configuration of a truss spar (Li 2012)

Table 1 Main characteristics of the spar

Properties	Units	Value
Water Depth	m	1524
Draft	m	154
Center of Buoyancy from Keel	m	112.34
Center of Gravity from Keel	m	91.27
Topside Payloads	ton	10770
Hull Weights	ton	14800
Total Displacement	ton	59250
Hard Tank Diameter	m	30
Length Overall	m	169
Hard Tank Length	m	74
Soft Tank Length	m	14
Truss Length	m	81
Truss Spacing	m	20
Fairlead Location from Keel	m	98

The mooring system of 'Constitution' consists of three groups, each of which has three mooring lines. Each mooring line has three segments: platform chain, mid-section cable, and ground chain. The riser system consists of 2 SCRs and 6 TTRs. The physical properties of mooring lines and SCRs are listed in Tables 2 and 3 respectively. The arrangement of the mooring system and riser system is shown in Fig. 3.

The detailed physical properties of TTR are not available to the authors. We assumed that double-casing risers are used due to the fact that only double-casing risers could be applied in this ultra-deep water condition. The size of this type of TTRs is sketched in Fig. 4.

Table 2 Mooring line properties

	Platform Chain	Mid-section	Ground Chain	Units
Line Type	R4 Studless	Steel Wire	R4 Studless	
Equivalent Diameter	0.142	0.127	0.142	m
Jacket Thickness		0.011		m
Weight in Air	3949.4	823.2	3949.4	N/m
Weight in Water	3439.8	646.8	3439.8	N/m
EA	152,957	151,020	152,957	ton

Table 3 SCR properties

	SCR #1	SCR #2	Units
Length	1706.88	1706.88	m
Diameter	0.254	0.3048	m
Dry Weight	561.54	958.4	N/m
Unit Buoyancy	511.46	736.5	N/m

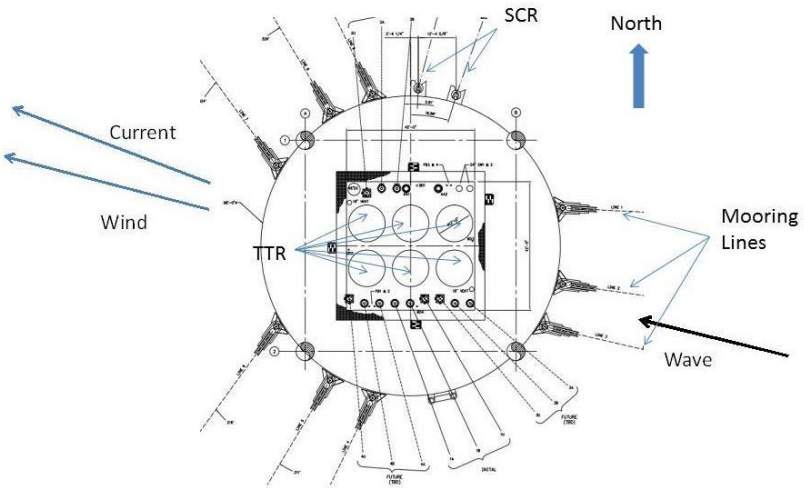

Fig. 3 Distribution of mooring lines and risers and headings of wave, wind and current

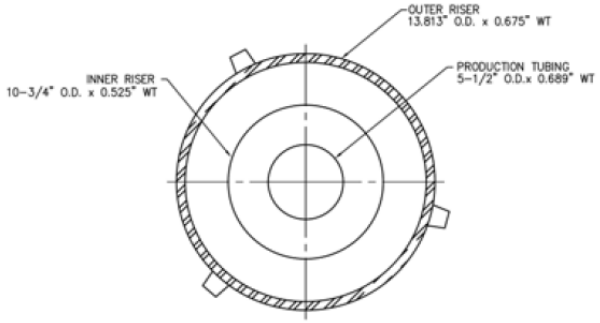

Fig. 4 Riser sizing of TTR case (cited from report from FloaTEC, 2009)

For quantifying the effects of tensioner systems and riser guides on the motion of the spar, we considered two different cases in our numerical simulation. In the first case, the six TTRs are tensioned by buoyancy cans, and in the second case, they are tensioned by tensioner systems. Since the water depth of 'Constitution' is similar with that of a case from an online report of FloaTEC (*RPSEA CTR 1402,* 2009*)*, the tensioner system from that report is adopted in our study. It consisted of four tensioner cylinders, each of which has a stiffness of 91.2 kN/m. The top tension is approximated as 1.5 times of the net dry weight of individual TTR and the approximate tension of each tensioner is 1650 kN.

3.2 Hydrodynamic coefficients used in the simulation

Magee *et al.* (2000), Prislin *et al.* (2005) and Theckumprath (2006) made attempts to quantify the hydrodynamic coefficients of the spar used in the Morrison Equation to calculate the inertia and drag forces applied on the spar. Their results are used in our simulation (See Table 4).

Table 4 Hydrodynamic coefficients

Spar Sections	Hydrodynamic Coefficient	
	Added-mass Coefficient	Drag Coefficient
Hard Tank	1	1.12
Truss Members	0.8	1
Soft Tank	1	1.12
Heave Plate	2	6
Mooring Chain	2	2.4
Mooring Wire	1	1.2

Table 5 Met-ocean data of hurricane 'Ike'

Load	Parameters	Units	Hurricane 'Ike'
Wave	Spectrum Type		JONSWAP
	Significant Height	meter	9.30
	Peak Period	second	14.84
	Shape Factor		2.20
	Heading	degree	170.00
Wind	Spectrum Type		API
	Speed	m/s	37.40
	Heading	degree	170.00
Current	Heading	degree	164.00
	Depth-Speed	m-m/s	0-0.8
			61-0.43
			92-0.1
			1524-0.05

3.3 Met-ocean conditions

Hurricane 'Ike' occurred on September 12th, 2008. The direction and magnitude of the wind, wave and current used in our simulation are presented in Table 5 and their headings are visualized in Fig. 3. For more detailed information of the met-ocean conditions of 'Ike', readers are referred to Kiecke (2011) and Li (2012).

4. Comparison of simulated results to field measurements

The dynamics of 'Constitution' is simulated using the extended COUPLE during one of the peak hours of 'Ike'. Three different versions of modeling TTRs connected to 'Constitution' were considered in the simulation. Otherwise, the modeling of 'Constitution' in the three versions is

identical. The duration for each simulation lasts 2048 seconds.

Version 1: TTRs are simplified as vertical constant force on the spar based on their wet weight.
Version 2: TTRs are tensioned by buoyancy cans with the flex joints at their bottoms. Each TTR is restrained by two riser guides.
Version 3: TTRs are tensioned by tensioner systems and have the flex joints at their bottoms. Same as Version 2, each TTR is restrained by two riser guides.

At first, static simulation of the spar was made to determine the equilibrium position of the spar under the combined impact of steady wind and currents, and mean wave drift forces. When the spar moves from the old equilibrium position (in the absence of wind, current and wave) to the new equilibrium position, the TTRs are experiencing the forces applied by the hull through the riser guides and tensioner systems. Inversely, the hull is also experiencing the reaction force from the TTRs, which may have influence on the new equilibrium position of the hull. Comparison will be made among the simulated results based on the three versions and field measurements (FM). FM data were detailed in Li (2012).

In Version 1 of the spar, only the wetted weight of TTRs is counted and the dynamic interaction between them and hull are neglected. In Version 2, the coupling effects at upper deck, riser guides and SCR flex joints are considered. It is noted that the dynamic effects of the TTRs on the heave of the spar are neglected due to the use of buoyancy cans. In Version 3, the TTR may apply significant dynamic vertical force on the hull through the tensioner systems. Hence, the comparison between the results of Version 1 and 2 may reveal the effects of riser guides and the comparison between the results of Version 2 and 3 may shed lights on the effects from tensioner systems.

4.1 Translation motion

Fig. 5 compares the translation motions simulated based on the three versions of the spar. To ensure clearness, only the results of first 1000-second simulation are plotted and it should be noted that the ramp function is applied for the first 100-s simulation.

4.1.1 Effects of riser guides

The surge and sway of the spar are quite synchronized but between the curves of Version 1 and Version 2 there are certain discrepancies, which are attributed to the effects of riser guides (See Fig. 5).

For the surge motion, the comparison between the results of Version 1 and Version 2 shows that the mean shift surge of Version 1 is about 3.3 m greater than that of Version 2, which also causes the corresponding differences in maximum and minimum displacements (See Table 6). The difference in Standard Deviation (SD) is insignificant. A similar trend is observed in the sway motion.

For the heave motion, the heave SD reduces from 0.59 m in Version 1 to 0.52 m in Version 2 and the difference is little. It is because that the TTRs tensioned by buoyancy cans are decoupled from the hull in vertical direction. The small reduction may be due to coupling effect between heave and other motion modes. Overall, TTRs tensioned by buoyancy cans have limited effects on the heave motion of the spar.

4.1.2 Effects of tensioner system

It is observed in Fig. 5 that the results of Version 2 and Version 3 are almost coincident with each other in the surge and sway motions. It indicates that the tensioner systems do not affect the horizontal motions substantially, which is further confirmed by comparing their related statistics, such as the maximum, minimum, mean and SD. Their differences are mostly within 3% (See Table 6).

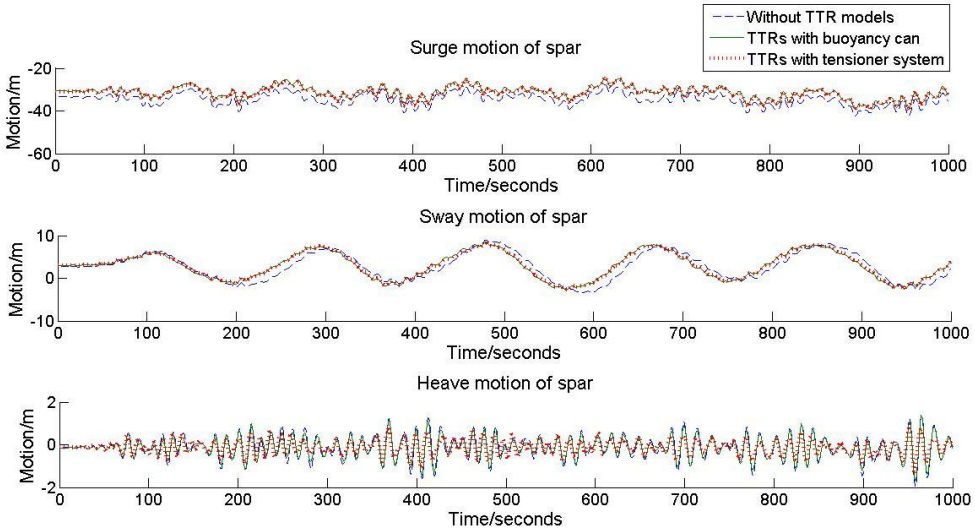

Fig. 5 Comparison in surge, sway and heave motions

Table 6 Statistics of simulated translation motions and field measurements

Direction	Statistics	Without TTR models (Version 1)	TTRs with Buoyancy Can(Version 2)	TTRs with Tensioner System (Version 3)	Field Measurement
Surge	Mean(m)	-34.379	-31.056	-31.465	-40.000
	Max(m)	-26.724	-24.252	-24.584	-27.200
	Min(m)	-46.826	-43.922	-44.085	-54.300
	SD(m)	2.871	2.949	2.863	3.000
Sway	Mean(m)	2.854	3.093	3.117	3.000
	Max(m)	9.043	9.574	9.298	9.500
	Min(m)	-3.395	-2.669	-2.605	-4.000
	SD(m)	3.339	3.273	3.199	2.800
Heave	Mean(m)	-0.104	-0.114	-0.122	-0.100
	Max(m)	1.462	1.366	0.846	1.000
	Min(m)	-2.321	-2.097	-1.531	-1.100
	SD(m)	0.596	0.525	0.380	0.300

However, the heave oscillation of Version 3 reduces significantly, when tensioner systems replace the buoyancy cans (See Table 6). When the tensioner systems are used to tension the TTRs, the tensioners apply dynamic vertical restoring forces to the hull in a manner to restrain the heave of the hull, and thus its heave SD is significantly reduced. In other words, the tensioner systems increase the vertical restoring stiffness of the floating system. The comparison in Table 6 shows that the maximum heave of Version 3 decreases by about 38.1% while the minimum increases by about 27.0%. The reduction in the heave SD of Version 3 is about 27.6%.

4.1.3 Comparison with the FM

It was noted that when wind, wave and current were insignificant before the hurricane 'Ike' reached the site of 'Constitution', the center of the spar was not locating at (0,0) (Li 2012). On the other hand, the origin of the spar is always located at (0, 0) in our simulation in the absence of wind, wave and current. The discrepancies between the two origins may result in the discrepancies in the maximum, minimum and mean between the FM and simulation in the presence of 'Ike'. Hence, our attention focuses on the comparison of the related SD values between the numerical results and FM.

The surge SD is respectively 2.95 m and 2.86 m for the simulation of Version 2 and 3 (See Table 6). The differences with respect to FM surge SD are within 5%. For the sway motion, both simulated SDs based on Version 2 and 3 are about 10% bigger than FM SD. The relatively large differences in the sway SD values may mainly result from the errors in the measured directions of wind. It is noted the heave SD based on Version 2 (TTRs tensioned by buoyancy cans) is about 50% greater than that of FM since the friction between riser and guides is neglected. The heave SD based on Version 3 is 0.38 m, which is very close to that of the corresponding measurements.

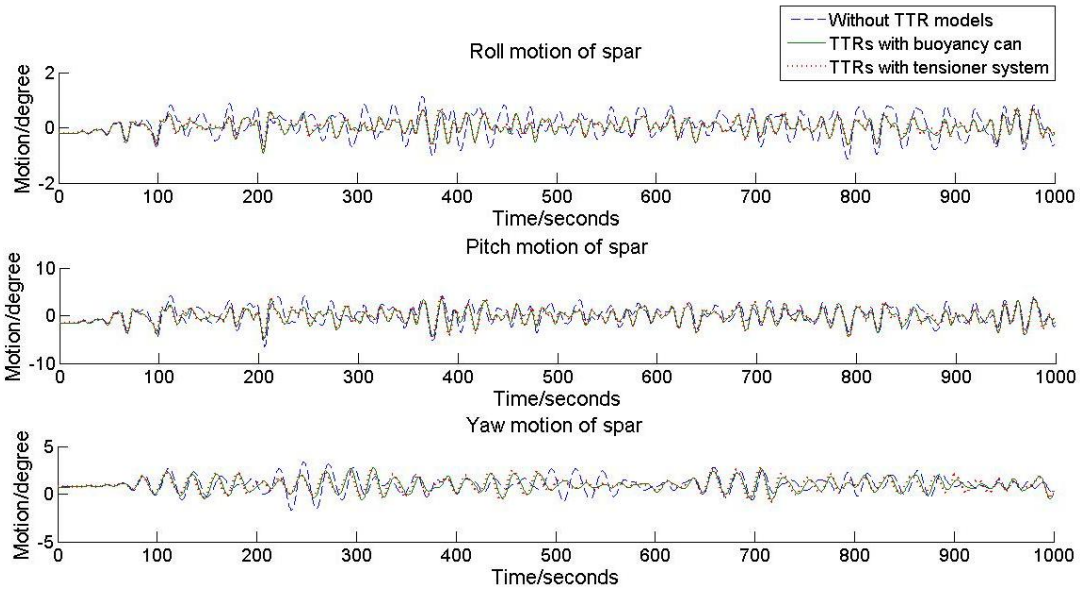

Fig. 6 Comparison in roll, pitch and yaw motions

Table 7 Statistical analysis on rotation motions and comparison with field measurements

Direction	Statistics	Without TTR models (Version 1)	TTRs with Buoyancy Can(Version 2)	TTRs with Tensioner System (Version 3)	Field Measurement
Roll	Mean(deg)	0.118	0.055	0.053	-0.100
	Max(deg)	1.316	0.766	0.843	1.200
	Min(deg)	-1.350	-0.944	-1.036	-2.100
	SD(deg)	0.470	0.266	0.271	0.400
Pitch	Mean(deg)	0.292	-0.049	-0.014	-2.000
	Max(deg)	5.798	4.823	5.128	0.400
	Min(deg)	-6.452	-6.044	-6.328	-7.000
	SD(deg)	1.794	1.552	1.581	1.500
Yaw	Mean(deg)	1.018	0.983	0.993	0.100
	Max(deg)	3.417	3.153	3.246	3.200
	Min(deg)	-1.685	-1.209	-1.279	-3.000
	SD(deg)	0.834	0.719	0.747	0.900

4.2 Rotational motion

4.2.1 Effects of riser guides

The comparison in Table 7 shows that the roll SD based on Version 2 is about 43.4% smaller than that based on Version 1. Similarly, the pitch SD based on Version 2 is also 13.4% smaller than that based on Version 1. The smaller roll and pitch SD values based on Version 2 indicate the spar rotational stiffness is strengthened owing to the consideration of the riser guides contacting TTRs (Koo *et al*. 2004). The changes in the natural frequencies will be discussed in subsection 4.3.

4.2.2 Effects of tensioner system

The roll and pitch results simulated respectively based on Version 2 and 3, are very close as shown in Fig. 6. The related statistics given in Table 7 also confirms the observation made based on Fig. 6. Both comparisons indicate that the rotational motions are not affected substantially when the buoyancy cans are replaced by tensioner systems.

4.2.3 Comparison with FM

In comparison with FM, as reasons explained in the subsection 4.1.3, we focus all attention to the SD values instead of the maximum, minimum and mean values. The simulated SD values agree reasonably well with those of FM especially for the pitch SD, which is the dominant rotation in the case of ‘Ike’ (See Table 7). The pitch SD values simulated based on Version 2 and 3 are 4% and 5% greater than that of FM, respectively. In terms of roll and yaw rotation, the simulated SD values are about 30% smaller than measurements; however it should be noted that the magnitudes of roll and yaw are much smaller than that of pitch.

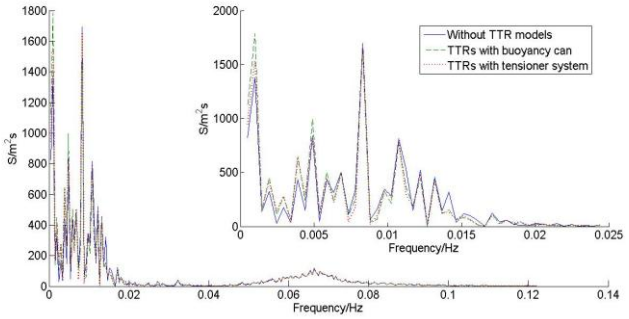

(a) Surge

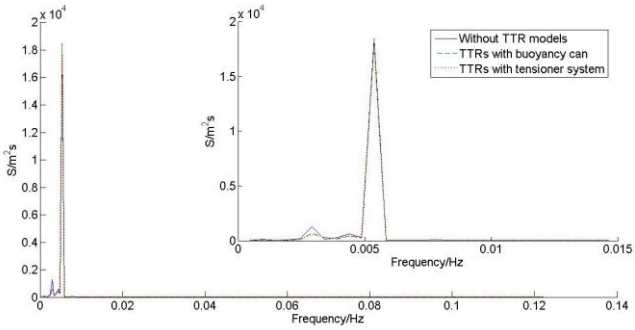

(b) Sway

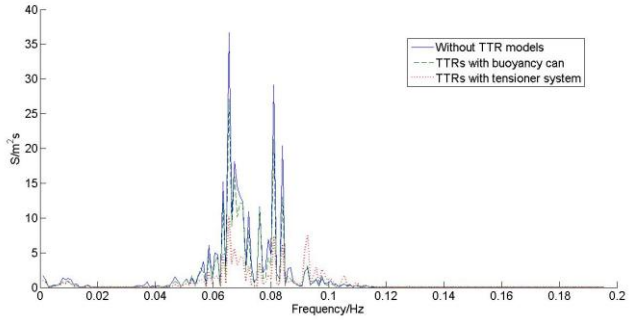

(c) Heave

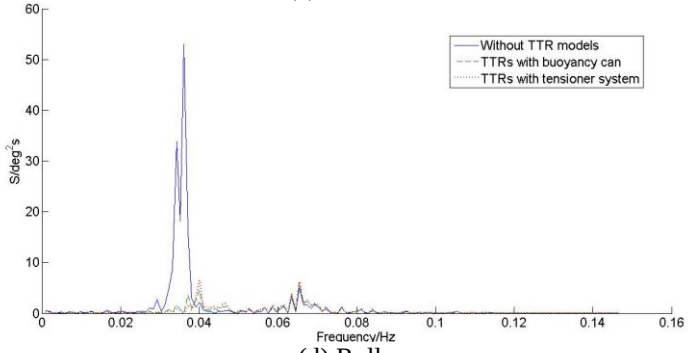

(d) Roll

Continued -

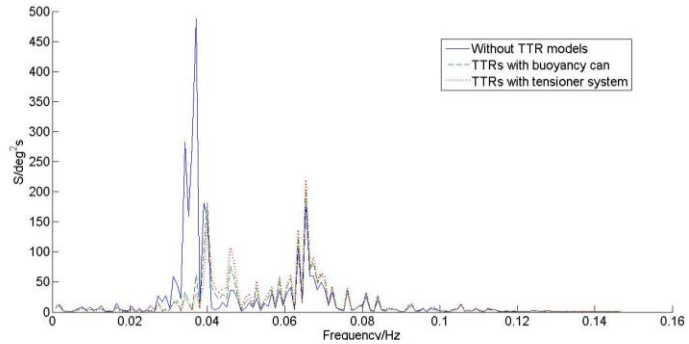

(e) Pitch

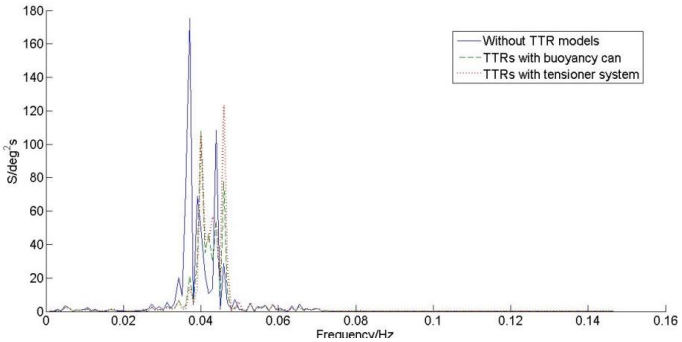

(f) Yaw

Fig. 7 Comparison of 6DOFs spectrum during the peak hours of 'Ike'

4.3 Power spectra of motions

Graph (a) in Fig. 7 shows that the three spectra of the surge simulated based on the three versions of the TTRs almost overlap with each other, in both low frequency range (<0.02 Hz) and the wave frequency range (0.05~0.08 Hz). The slow-drift surge is dominant, which is typical for a spar and expected. The natural frequencies of the spar simulated based on the three different versions of the TTR do not show any noticeable difference, indicating the inclusion of the riser guides and tensioner systems does not significantly alter the related natural frequency. Similar observation is made in the comparison of Sway spectra (See Graph (b) in Fig. 7) although the energy in the sway motion is much smaller.

The comparison presented in Graph (c) of Fig. 7 reveals that the heave spectra simulated respectively based on Version 1 and Version 2 are similar and the heave energy concentrates on the wave frequency range. The above observation indicates the TTRs tensioned by buoyancy cans do not have significant impact on the heave motion since they are decoupled from the spar motion in vertical direction. However, the heave spectrum simulated based on Version 3 shows that the heave motion is substantially reduced in comparison with those based on Version 1 and 2, which is consistent with the observation made in the comparison of heave SD values.

It is observed that the natural frequencies of the rotational motions increase when allowing for the effects of riser guides and tensioner systems in the simulation. The natural frequencies of the roll and pitch simulated based on Version1 are about 0.038 Hz (See graph (d) and (e) of Fig. 5.8). Yet, after the effects of the riser guides and tensioner systems on the TTRs are considered in the

simulation (Version 2 and 3), the peaks in the related spectra shift to around 0.04 Hz. The increases in these natural frequencies are due to the contributions of the TTRs which strengthen the rotational stiffness of the spar.

5. Conclusions

The existing code CABLE3D is extended to allow for the numerical simulation of the TTRs, which are tensioned by the tensioner systems or buoyancy cans at the top, constrained by the riser guides at elevations near the water surface and connected by flex joints at their bottoms. The extended CABLE3D is then integrated into COUPLE, making COUPLE capable of simulating a floating system interacting with TTRs and SCRs. Using the extended COUPLE, the motions of 'Constitution', a truss spar, are simulated under the impact of Hurricane 'Ike' and the analysis of effects of the tensioner systems, riser guides are conducted. The main conclusions based on this study are summarized below.

1. The riser guides do not affect the surge and sway motion substantially. The heave motion decreases significantly in the case of the TTRs tensioned by the tensioner systems. The decrease in the heave is mainly due to the increase in the heave stiffness of the spar resulting from the interaction of the spar and TTRs through the tensioner systems.
2. The rotational motions of the spar, especially roll and pitch, are significantly reduced when the interaction between the hull and TTRs through the riser guides are included in the simulation. Due to the extra horizontal support provided by the TTRs through the riser guides, the rotational stiffness of the hull increases and in turn the rotational natural frequencies increase.

Acknowledgements

The authors would like to thank ABS for the financial support of this project and Anadarko for providing the measurements of 'Constitution' during Hurricane of 'Ike'.

References

API Recommended Practice 2RD (2006), *Design of Risers for Floating Production Systems (FPSs) and Tension-Leg Platforms (TLPs)*, American Petroleum Institute, Washington, DC.

Cao, P.M. and Zhang, J. (1997), "Slow motion responses of compliant offshore structures", *Int. J. Offshore Polar*, **7**(2), 119-126.

Chen, C.Y., Kang, C,H. and Mills, T. (2008), "Coupled spar response with buoyancy cans vs. Tensioners", *Proceedings of the 18th International Offshore and Polar Engineering Conference*, Vancouver.

Chen, C.Y. and Nurtjahyo, P. (2004), "Numerical prediction of spar motions considering top tension riser stiffness", *Proceedings of the OMAE04, 23rd International Conference on Offshore Mechanics and Arctic Engineering*, Vancouver.

Chen, X.H. (2002), *Studies on dynamic interaction between deep-water floating structure and their mooring/tendon systems*, PhD thesis, Texas A&M University, US.

FloaTEC, RPSEA CTR 1402 (2009*), Ultra deepwater dry tree system for drilling and production in GOM*, Stage 1 Study Report, June 19 2009, FloaTEC project# 08110.

Garrett, D.L. (1982), "Dynamic analysis of slender rods", *J. Energ. Resour – ASME*, **104**, 302-307.

Kiecke, A.F. (2011), *Simulated fatigue damage index on mooring lines of a Gulf of Mexico truss spar determined from recorded field data*, MS Thesis, Ocean Engineering Program, Civil Engineering Department, Texas A&M University, US.

Kim, M.H. and Chen, W. (1994), "Slender-body approximation for slowly-varying wave loads in multi-direction waves", *Proceedings of the 6th Offshore and Polar Engineering Conference*.

Koo, B.J., Kim, M.H. and Randall, R. (2004), "The effects of nonlinear multi-contact coupling with gap between risers and guide frame on global spar motion analysis", *Ocean Eng*., **31**, 1469-1502.

Li, C.X. (2012), *Coupled analysis of the motion and mooring loads of a spar 'Constitution'*, MS Thesis, Ocean Engineering Program, Civil Engineering Department, Texas A&M University, US.

Ma, W. and Webster, W.C. (1994), *An analytical approach to cable dynamics: theory and user manual*, Sea Grant Project R/OE-26.

Magee, A., Sablock, A., Maher, J., Halkyard, J., Finn, L. and Dutta, I. (2000), "Heave plate effectiveness in the performance of the truss spar", *Proceedings of the ETCE/OMAE2000 Joint Conference on Energy for the New Millennium*, New Orleans.

Morison, J.R., O'Brien, M.P., Johonson, J.W. and Shaaf, S.A. (1950), "The forces exerted by surface waves on plies", *Petrol. Trans. AIME*, **189**, 149-154.

Murray, J., Tahar, A. and Yang, C.K. (2007), "Hydrodynamics of dry tree semisubmersible", *Proceedings of the ISOPE'07*, Lisbon.

Murray, J., Tahar, A. and Eilertsen, T. (2006), "A comparative assessment of spar, tension leg platform and semisubmersible floaters for deepwater application", *Proceedings of the DOT International Conference and Exhibition*.

Perryman, S., Gebara, J., Botros, F. and Yu, A. (2005), *Holstein truss spar and top tensioned riser system design challenges and innovations*, OTC 17292.

Prislin, I., Rainford, D., Perryman, S. and Schilling, R. (2005), *Use of field monitored data for improvement of existing and future offshore facilities*, SNAME Paper D5.

Webster, R.L. (1975), "Non-linear static and dynamic response of underwater cable structures using finite element approach", *Proceedings of the 7th Offshore Technology Conference*, Houston.

Webster, W.C. (1995), "Mooring induced damping", *Ocean Eng*., **22**, 57-591.

Yang, C.K and Kim, M.H. (2010), "Linear and nonlinear approach of hydropneumatic tensioner modeling for spar global performance", *J. Offshore Mech. Arct*., **132**(1).

Yang, C.K and Kim, M.H. (2011), "The structural safety assessment of a tie-down system on a tension leg platform during hurrycane events", *Ocean Syst. Eng*., **1**(4), 263-283.